Noncovalently Connected Polymeric Micelles Based on a Homopolymer Pair in Solutions

Min Wang, Guangzhao Zhang, Daoyong Chen, Ming Jiang,* and Shiyong Liu

Department of Macromolecular Science and The Key Laboratory of Molecular Engineering of Polymers (Ministry of Education, China), Fudan University, Shanghai 200433, P. R. China

Received April 3, 2001; Revised Manuscript Received July 3, 2001

ABSTRACT: The intermolecular complexes with poly(4-vinylpyridine) (PVPy) as the backbone and carboxyl-terminated polybutadiene (CPB) as the grafts were formed due to hydrogen bonding in their common solvent chloroform. Two solvent pairs, i.e., *n*-hexane/chloroform and nitromethane/chloroform, were found selective for CPB and PVPy, respectively. Thus, the stable micelles with PVPy being the core and CPB being the shell, denoted as (PVPy)−CPB, and the ones with CPB core and PVPy shell, denoted as (CPB)−PVPy, were formed in the corresponding selective solvent pairs. Differing from the conventional micelles made of block or graft copolymers, the present micelles possess hydrogen bonds instead of covalent bonds connecting the core and shell and their composition; i.e., the weight ratio of the core to shell is readily adjustable. Dynamic light scattering study demonstrated that the average hydrodynamic diameters $\langle D_h \rangle$ of the micelles were mostly in the range from 100 to 300 nm depending on the solvent composition, polymer concentration, and the chain number ratio of CPB to PVPy, etc. (PVPy)−CPB were found more stable against dilution than (CPB)−PVPy. The two kinds of micelles differ in their diameter−composition dependence; namely, with increasing the ratio of CPB/PVPy, $\langle D_h \rangle$ of (PVPy)−CPB decreases monotonically while that of (CPB)−PVPy increases at the low ratio range but decreases at the high ratio range. Besides, the core−shell structure of both micelles was clearly visualized by transmission electronic microscopy using staining techniques.

Introduction

Most of polymeric micelles reported in the literature are made of block or graft copolymers in *selective* solvents.[1−4] Efforts have recently been made to produce micelles via different pathways. For example, in a nonselective solvent, a block copolymer can form micelles when one of its blocks complexes with a homopolymer due to ionic interaction,[5,6] and chemical modification of one block of a block copolymer can also lead to the formation of polymeric micelles.[7] As a first example, our laboratory reported micellization of a block copolymer and a random copolymer in a nonselective solvent caused by interpolymer hydrogen-bonding complexation.[8]

In all the polymeric micelles reported, the core and shell (corona) are connected by chemical bonds. Our recent work has been devoted to self-assembly of homopolymer or homopolymer/copolymer pairs into micelles due to intermolecular hydrogen bonding.[9−12] Such micelle-like structure is characterized by hydrogen bonds instead of covalent bonds connecting the core and shell. As an example, we reported that carboxyl-ended polystyrene oligomer and poly(4-vinylpyridine) (PVPy) formed "graft" copolymers in common solvent due to the hydrogen bonding between the carboxyl and pyridine units.[10] Furthermore, the graft copolymers assembled into micelles in a selective solvent for PS grafts.[11] This result stimulated our interests to explore such noncovalently connected micelles systematically with emphasis on their formation, stability, morphology, and the dependence of the micelle structure on the composition and parameters of the component polymers. Here we report "grafting" of carboxyl-ended polybutadiene (CPB) into PVPy in a common solvent and their micellization in two solvent mixtures, selective for CPB and PVPy, respectively. Thus, we are able to compare the structure and behavior between the micelles with PVPy as the core and CPB as the shell and those with CPB core and PVPy shell. For convenience, the former is denoted as (PVPy)−CPB while the latter (CPB)−PVPy.

The micelles of graft copolymers in which the backbone and grafts are linked by chemical bonds can be regarded as counterparts of our noncovalently connected micelles. However, compared to block copolymers, much fewer studies on micellization of graft coplymers were reported. In recent years, Kikuchi and Nose[13,14] studied aggregation of poly(methyl methacrylate-*g*-polystyrene) forming flowerlike and rodlike unimolecular and multimolecular micelles, respectively, in the selective solvents for the backbone and grafts. Webber et al. reported micellization of graft copolymers with poly(styrene-*alt*-maleic anhydride) (PSMA) backbone and poly(ethylene oxide) (PEO) grafts[15] and those with poly(acrylic acid) (PAA) backbone and polystyrene (PS) grafts.[16] Micellization in water selective for PEO grafts in the former and PAA backbone in the latter was studied with emphasis on the structure and properties of the micelles and their dependences on the copolymer parameters.

Although in this paper we concentrate on the micellization of homopolymer pairs with interpolymer hydrogen bonding in solutions, it should be mentioned that the supramolecular structure and properties of polymer-containing systems with hydrogen bonding in the solid state have received much attention in the literature for years. For example, some polymer−surfactant or polymer−amphiphile supramolecules formed due to hydrogen bonding, leading to highly ordered morphologies such as hexagonal cylindrical[17] and lamellar structures.[18] In addition, a widely variety of self-assembled supramolecular liquid-crystalline structures have been

* To whom correspondence should be addressed.

10.1021/ma0105845 CCC: $20.00 © 2001 American Chemical Society
Published on Web 08/21/2001

reported through the formation of hydrogen bonds between different and independent components.[19−22]

Experimental Section

Sample Preparation. Carboxyl-terminated polybutadiene was prepared by free-radical polymerization of butadiene initiated by succinic peroxide in solution. Most of the resultant polybutadiene chains carried carboxyl groups at both ends as the combination termination of the propagating free-radical dominated. The carboxyl content was determinded to be 0.561 mmol/g, and hence the calculated molecular weight was 3565. Poly(4-vinylpyridine) was synthesized and purified as described.[10] The viscosity-average molecular weight M_η of PVPy was 1.4×10^5, and the weight-average molecular weight measured by static light scattering was 2.3×10^5.

Viscosity Measurements. Reduced solution viscosity measurements were made with an Ubbelodhe viscometer at 30.0 ± 0.1 °C in chloroform with a total polymer concentration of 8.0 mg/mL. The blend solutions with different compositions were prepared by mixing solutions of CPB and PVPy as desired.

Laser Light Scattering (LLS). A commercial laser light scattering (LLS) spectrometer (Malvern Autosizer 4700) equipped with a multi-τ digital time correlation (Malvern PCS7132) and a solid-state laser (ILT 5500QSL, output power = 100 mW at λ_0 = 514.5 nm) as light source was used. In dynamic LLS, i.e., DLS, the line-width distribution $G(\Gamma)$ can be calculated from the Laplace inversion of intensity−intensity−time correlation function $G^{(2)}(q,t)$.[23] The inversion was carried out by the CONTIN program supplied with the Malvern PCS7132 digital time correlator. $G(\Gamma)$ can be converted into a transitional diffusion coefficient distribution $G(D)$ or a hydrodynamic radius distribution $f(D_h)$ via the Stokes−Einstein equation, $D_h = (k_B T/3\pi\eta)D^{-1}$, where k_B, T, and η are the Boltzmann constant, the absolute temperature, and the solvent viscosity, respectively. All the DLS measurements were done at 30.0 ± 0.1 °C and at a scattering angle 90° as only a little scattering angle dependence of the $\langle D_h \rangle$ of the micelle was observed. Except the cases of studying concentration and composition dependence, all the samples with a total polymer concentration of 0.1 mg/mL were used. The solutions were clarified using a 0.45 μm Millipore filter before the measurements, except the solutions with micelle size larger than 250 nm.

Transmission Electron Microscopy (TEM). Transmission electron microscopy was used to observe the morphologies of the particles. Dilute CPB/PVPy 10/1 (w/w) micelle solutions with a total polymer concentration of 0.275 mg/mL were used for specimen preparation on copper grids coated with a thin carbon film. The specimens were stained with the vapor of osmium tetroxide (OsO_4) 1% (w/w) water solution after solvent evaporation. TEM observations were performed on a Philips CM 120 electron microscope at an accelerating voltage of 80 kV.

Results and Discussion

Soluble "Graft Copolymer" and Its Micellization. The carboxyl end groups in CPB are expected to interact with pyridine units in PVPy, leading to "grafting" of CPB to PVPy backbone due to hydrogen bonding. This speculation was confirmed by viscosimetry and light scattering studies. Viscometry is a simple and effective technique for monitoring complexation of polymer blend solutions. Generally, if no specific interactions exist in a polymer pair, the reduced viscosity of the polymer pair is close to the additivity law of the component viscosity. However, positive[24−29] or negative[24,30] deviation from the additivity law may occur if specific interactions between the polymer pair are strong enough, suggesting intermacromolecular complexation. Figure 1 shows the reduced viscosities of the CPB/PVPy blend solutions vs the weight fraction of CPB. Over the whole composition

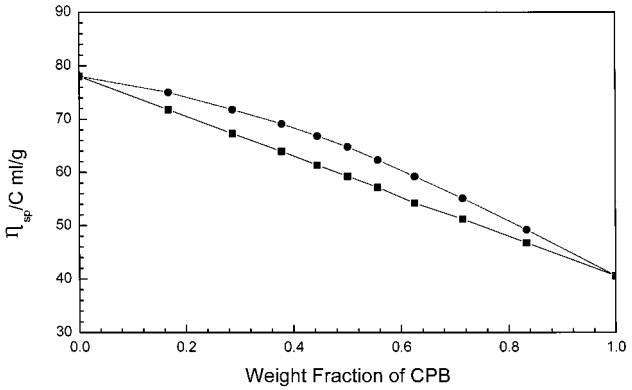

Figure 1. Reduced viscosity of the blend of PVPy and CPB in chloroform as a function of weight fraction of CPB: (●) experimental value; (■) calculated value by additivity law. The total concentration of the polymers is 8.0 mg/mL.

range, the blend solutions kept their transparency, but their reduced viscosities presented a substantial positive deviation from the additivity law. It clearly showed that the individual polymer chains combined together forming large species, i.e., soluble graftlike complexes in chloroform. In addition, DLS measurements for pure PVPy in chloroform presented a $\langle D_h \rangle$ of 40 nm but no accurate value for CPB as the chains were too small to give rise to enough scattering intensity. For the blend solutions with compositions of CPB/PVPy 5/1 (w/w) and 10/1 (w/w), the $\langle D_h \rangle$ values were found to be 66 and 70 nm, respectively. This significant increase of $\langle D_h \rangle$ compared to that of pure PVPy clearly showed the "grafting" of CPB onto PVPy backbone. As in the solutions over the whole composition range no gelation occurred, we concluded that the "graft" copolymers were soluble although there were carboxyl groups at both ends in each CPB chain.

Both CPB and PVPy can be dissolved in chloroform. Hexane is a nonsolvent for PVPy, as precipitation occurred quickly when 2 mL of hexane was added to 10 mL of PVPy chloroform solution. Polybutadiene without carboxyl groups can be readily dissolved in hexane, but CPB cannot probably because of its intermolecular association. However, CPB kept soluble even in the solvent mixture of hexane/chloroform 99/1 v/v. Therefore, chloroform/hexane may serve as a selective solvent mixture for CPB. As hexane was added dropwise into the solutions of CPB/PVPy (10/1, w/w) in chloroform, the solution kept completely colorless and transparent until the volume ratio of hexane/chloroform reached around 3/7 when the solution turned to be slightly bluish. Adding more hexane did not cause precipitation. This means that the collapsed and aggregated PVPy chains were stabilized by the solvated short CPB chains due to hydrogen bonding between them. DLS measurements were performed for the solutions of CPB/PVPy (10/1, w/w) in hexane/chloroform with different compositions ranging from 3/7 to 99/1 (v/v). To prepare the micelle solution, CPB and PVPy solutions in chloroform were mixed at a desired weight ratio and followed by adding hexane dropwise very slowly to the solutions. For producing the micelle solutions in the solvent mixture with the extreme composition, i.e., hexane/chloroform 99/1 (v/v), alternatively, a desired amount of CPB/PVPy solution was added extremely slowly to hexane. The distribution curves of hydrodynamic diameter $f(D_h)$ of the blend solutions are shown in Figure 2. Compared with the $\langle D_h \rangle$ value in pure solvent (70 nm),

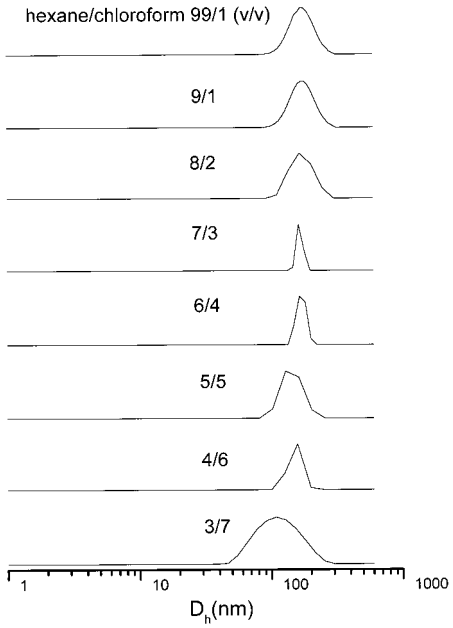

Figure 2. Hydrodynamic diameter distributions of CPB/PVPy (10/1, w/w) in hexane/chloroform with different volume ratio.

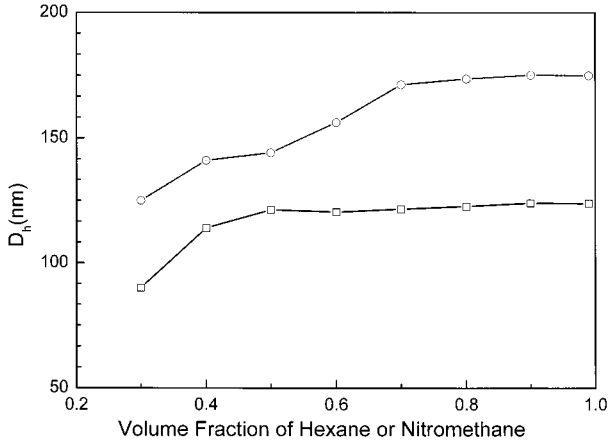

Figure 3. Average hydrodynamic diameters $\langle D_h \rangle$ of CPB/PVPy (10/1, w/w) as a function of hexane fraction in hexane/chloroform (⊙) and nitromethane fraction in nitromethane/chloroform (□).

much larger diameters (125−175 nm) were found in the solvent mixtures. Depending on the solvent composition, the polydispersity ($\mu_2/\langle\Gamma\rangle^2$) of the distribution varies in the range from 0.04 to 0.19. This result demonstrated the formation of (PVPy)−CPB composed of PVPy core and CPB shell. Figure 3 displays $\langle D_h \rangle$ of the micelles as a function of the solvent composition. Obviously, with increasing the hexane volume fractions from 0.3 to 0.7 and subsequently worsening the solvent quality to the PVPy chains, the micelle size increases. As the hexane fraction increases further, almost no size change is observed as the PVPy in such solvent mixtures totally loses its solvability.

Nitromethane was found to be a precipitant for CPB but a good solvent for PVPy, and its homologue 1-nitropropane was reported to have a little effect on the hydrogen bonding between carboxyl and pyridine.[31] Therefore, nitromethane/chloroform was chosen as a selective solvent mixture for producing (CPB)−PVPy composed of PVPy shell and CPB core. For the solutions of CPB/PVPy (10/1, w/w) in chloroform with continuing addition of nitromethane, bluish opalescence appeared

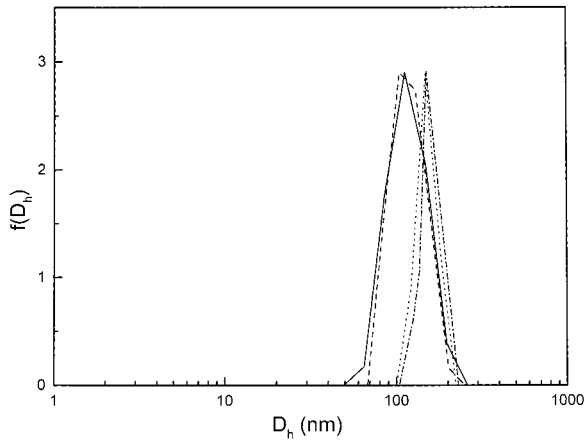

Figure 4. Hydrodynamic diameter distributions $f(D_h)$ of the micelles of CPB/PVPy (10/1, w/w) in nitromethane/chloroform (6/4, v/v) measured (—) 3 days and (---) 30 days after preparation and in hexane/chloroform measured (···) 3 days and (- · -) 150 days after preparation.

when the composition of nitromethane/chloroform reached 3/7 (v/v), indicating the formation of the micelles. No macroscopic precipitation was observed even in the solvent with an extreme high proportion of nitromethane (99.9%). Obviously, further aggregation of CPB into large precipitate in its poor solvent was prevented by the soluble PVPy chains that surrounded the aggregate. The DLS measurements for the micelles composed of CPB/PVPy (10/1, w/w) in the solvent mixture with the nitromethane volume fraction ranging from 0.3 to 0.99 indicated that the micelles possessed the polydispersity in the similar range as that of (PVPy)−CPB (data not shown). The average hydrodynamic diameters of (CPB)−PVPy as a function of the solvent composition are shown in Figure 3 as well. $\langle D_h \rangle$ shows an increase from 90 to 114 nm as nitromethane volume fraction goes up from 0.3 to 0.4. However, only a little change followed when nitromethane increased further. Compared to (PVPy)−CPB, the size of (CPB)−PVPy is significantly smaller at the same concentration (0.1 mg/mL) and composition (CPB/PVPy, 10/1, w/w).

Stability of Micelles vs Time and Concentration. Since in both kinds of micelles mentioned above the hydrogen bonds, connecting the core and shell, are sensitive to external conditions, the micelle stability in solution is worth exploring. The variation of $\langle D_h \rangle$ of (PVPy)−CPB with composition of CPB/PVPy (10/1, w/w) in hexane/chloroform (6/4, v/v), as a typical example, was traced by DLS. $\langle D_h \rangle$ values of the micelles, i.e., 156, 155, 158, and 157 nm, were obtained after 3, 14, 60, and 150 days after the micelle preparation, respectively. For clarity, only two curves of the micelles are shown in Figure 4. A similar result was obtained for (CPB)−PVPy; i.e., almost $\langle D_h \rangle$ did not change in an interval of 30 days. The two curves are shown in Figure 4 as well. The results clearly evidenced a very good stability of both kinds of micelles, although there are no chemical bonds connecting the core and shell.

Figure 5 shows $\langle D_h \rangle$ of both (PVPy)−CPB and (CPB)−PVPy as a function of polymer concentration. All the micelles with $\langle D_h \rangle$ shown in Figure 5 have the same composition CPB/PVPy 10/1 (w/w) in nonsolvent/chloroform 6/4 (v/v). The micelles with different concentrations were prepared by diluting the initial solutions with total concentration of 0.55 mg/mL for (PVPy)−CPB and 0.275 mg/mL for (CPB)−PVPy with the corresponding solvent mixtures.

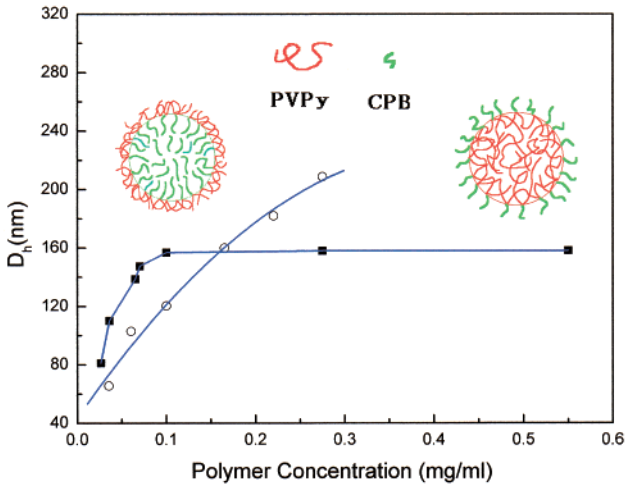

Figure 5. Polymer concentration dependence of $\langle D_h \rangle$ of (PVPy)−CPB (■) and (CPB)−PVPy (○) of CPB/PVPy (10/1, w/w) in nonsolvent/chloroform (6/4, v/v).

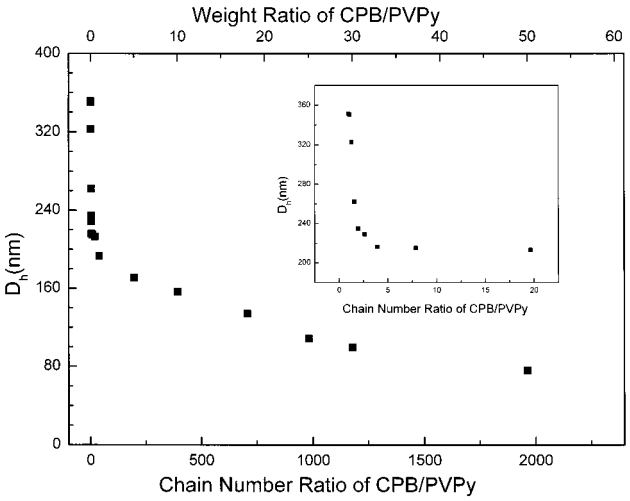

Figure 6. $\langle D_h \rangle$ of (PVPy)−CPB in hexane/chloroform (6/4, v/v) as a function of composition (chain number ratio and weight ratio of CPB to PVPy).

For (CPB)−PVPy with CPB grafts as the core, it was not possible to prepare stable micelle solutions with concentrations higher than 0.30 mg/mL, as the solutions turned to be milky white containing large aggregates. However, the micelle solutions with concentrations less than 0.30 mg/mL were stable. As shown in Figure 5, $\langle D_h \rangle$ of (CPB)−PVPy significantly depends on the polymer concentration. Specifically, $\langle D_h \rangle$ decreases from 208.8 to 65.6 nm as the concentration decreases from 0.275 to 0.0352 mg/mL. This significant $\langle D_h \rangle$ dependence is similar to that for PAA-*g*-PS micelles with PS grafts as the core.[16] It was reported that the $\langle D_h \rangle$ of PAA-*g*-PS in water was decreased from about 130 to 40 nm when the initial concentration of the polymer in dioxane varied from about 6.5 to 0.5 mg/mL. In addition, in the D_h distribution curve for (CPB)−PVPy solutions with the lowest concentration, besides the micelle peak at 66.5 nm a broad peak appeared around 1.6 nm, which indicated that the free polymer chains became detectable (curve not shown).

(PVPy)−CPB with CPB graft serving as the shell shows a different $\langle D_h \rangle$ dependence on concentration. A remarkable feature of the curve in Figure 5 is that there is a broad concentration range from 0.10 to 0.55 mg/mL, in which $\langle D_h \rangle$ almost does not change. In addition, for the micelle solutions prepared by an alternative way, i.e., adding hexane to solutions of CPB/PVPy in chloroform with different concentrations, almost the same $\langle D_h \rangle$ values were obtained as that shown in the plateau area in Figure 5. This means that in this concentration range the micelle size is insensitive to concentration as well as to the preparation procedures. However, when the solution was diluted further, the micelle size apparently decreased, but no signals associated with free polymer chains were detected, which is different from (CPB)−PVPy micelles.

The difference in the concentration dependence of the micelle size between the two micelles is of course associated with the difference in the micelle structures. As schematically illustrated in Figure 5, for (CPB)−PVPy, as the CPB chains are short and the micelles are as large as 100−200 nm, the core is actually composed of a large amount of CPB chains, and consequently only a small part of the chains, which locate in the surface area, are connected with PVPy chains. In the shell, each PVPy chain forms many loops anchored to the surface. As most of CPB chains do not have connection with the pyridine units in PVPy chains, the core is consequently not stable vs dilution, which is favorable to dissociation of the large CPB aggregates. In the case of (PVPy)−CPB, the short CPB chains are believed to have their end groups attached to the surface and the chains extend in solutions to stabilize the PVPy aggregate. As each PVPy chain has 10^3 pyridine units and the core size is in the same order as that of the PVPy molecules, we may imagine that most of the PVPy chains in the core has its own hydrogen-bonding sites connecting soluble CPB chains. Therefore, (PVPy)−CPB is much more stable vs dilution, except in the extremely low-concentration range.

Dependence of Micelle Size on Composition. Differing from the micelles of block or graft copolymers, our H-bond-connected micelles do not have a definite composition. In fact, the ratio of the number of chains in core to shell is readily adjustable. Therefore, we are able to investigate the composition effect on the size of the micelles. In all cases below no aggregates were seen when core-forming component is zero. (PVPy)−CPB in hexane/chloroform (6/4, v/v) over a broad range of compositions, i.e., CPB/PVPy from 0.025 to 50 in weight ratio and accordingly from 1 to 1960 in chain number ratio, were prepared, and their size distributions were studied by DLS. Figure 6 displays the dependence of $\langle D_h \rangle$ on composition. The main features of the result are as follows. First, the soluble grafts showed a remarkable ability to stabilize the PVPy aggregates as evidenced by the fact that micelles formed and kept stable even when the weight ratio CPB/PVPy was as low as 0.025, i.e., only one CPB chain on average for each PVPy chain. Second, in the low CPB/PVPy ratio range, the size of the micelles dramatically decreases with increasing the ratio. Specifically, $\langle D_h \rangle$ drops from 351.4 to 216.2 nm as the chain number ratio of CPB to PVPy varies from 1 to 4. Third, the dramatic drop is followed by a rather mild decrease. As shown in the insert, there is a break in the curve at the chain number ratio around 4. As found in many amphiphilic systems forming micelles or microparticles,[15,32,33] for a given system, the area that could be stabilized by each soluble species is nearly a constant. Our results here indicate that, at a high chain number ratio, one CPB chain is not able to stabilize the same area as that at a low chain number ratio. This

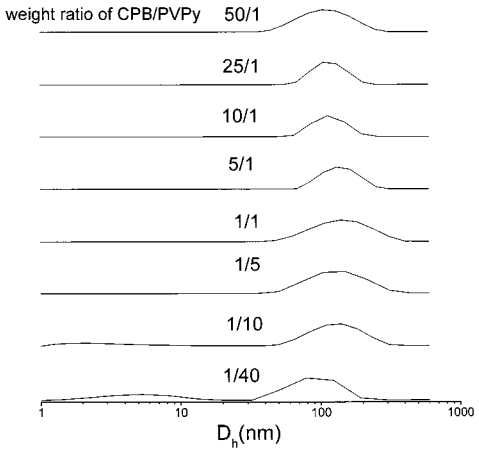

Figure 7. Some of D_h distributions of (CPB)−PVPy with different compositions in nitromethane/chloroform (6/4, v/v).

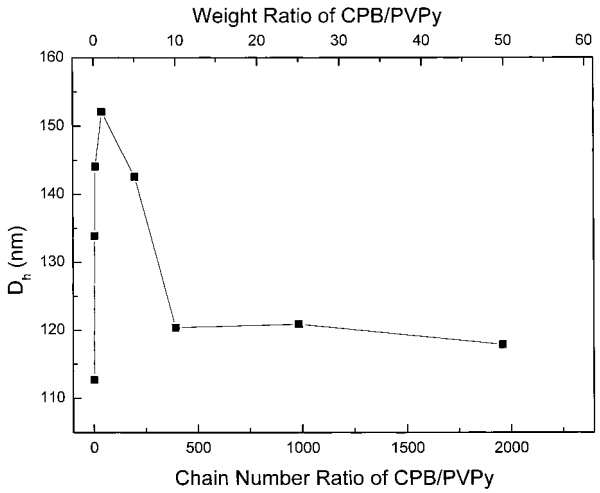

Figure 8. $\langle D_h \rangle$ of (CPB)−PVPy in nitromethane/chloroform (6/4, v/v) as a function of composition (chain number ratio and weight ratio of CPB to PVPy).

reflects the kinetically controlled nature of the CPB/PVPy micelles. In the highest ratio range, on average one PVPy chain possesses as many as 10^2-10^3 CPB grafts. Obviously, such a large number of CPB chains are too crowded to be located in the core−shell interface area, so double-layers and multilayers of CPB chains in the shell are quite possible. In the corresponding D_h distribution curve, species with diameter less than 10 nm appeared, indicating the presence of free component molecules (curve not shown).

Webber[15] reported micellization of graft copolymer PSMA-*g*-PEO in water, where the grafts served as shell component, just as our (PVPy)−CPB micelles. It was found that the micelle size decreases from 94 to 28 nm with increasing grafting density from 2.5 to 20. This dependence is quite similar to our present results of CPB/PVPy although in which there are no chemical bonds between the core and shell.

Figure 7 displays D_h distributions for (CPB)−PVPy at different CPB/PVPy ratio. Over the whole CPB/PVPy ratio range except the lowest one, the curves show one peak with the polydispersity varying within a range from 0.04 to 0.17. For the case of the lowest CPB/PVPy ratio of 1/40 and accordingly, on average only one CPB chain for one PVPy, in addition to the main peak, a very weak but broad one appeared at a very low $\langle D_h \rangle$ region, which can probably be associated with the free low molecular weight PVPy chains. Such PVPy molecules did not carry any grafts and kept as separated coils in solution when the micelle formed. Figure 8 depicts $\langle D_h \rangle$ vs the composition. Clearly, it shows opposite dependence of $\langle D_h \rangle$ on composition at the low and high CPB/PVPy ratio ranges. This result, in our opinion, can be rationalized as the result of competition between intermolecular and intramolecular aggregations. Both intermolecular and intramolecular aggregation result in micellization. However, the intramolecular process is accompanied by collapse and aggregation of the short branchs attached to the same backbone, which does not substantially affect the overall size. In contrast, the intermolecular process implies aggregation of the "graft" copolymers as building blocks, which of course results in a dramatic size increase. At the extreme low ratio, i.e., on average each "copolymer" backbone has one graft, the micelles formed possesses a diameter of 112.7 nm. As the graft number increases, the size continually increases up to its highest value of 152.1 nm when the chain number ratio of CPB to PVPy reaches 40. At this relatively low graft/backbone ratio range, the contribution of the intramolecular aggregation to micellization is small. Obviously, as the ratio increases, there are more and more possibilities for intramolecular aggregation. That is why $\langle D_h \rangle$ decreases with increasing the chain number ratio of CPB/PVPy in the high ratio range. In fact, for the micelles of poly(acrylic acid)-*g*-polystyrene in water[16] with core composed of PS grafts and shell of PAA backbone, it was found that the diameter decreased with grafting density just as we observed for the region with the chain number ratio of CPB/PVPy higher than 40. In addition, it was found that the intensity of scattered light of (CPB)−PVPy had the same dependence on composition as that shown in Figure 8.

Direct Observation of Micelle Morphologies. Transmission electron microscopy has been a powerful and efficient technique for revealing internal microstructure of polymeric micelles and microparticles. However, it is hard to see the core/shell structure if there is no enough natural contrast between the core and shell. Serizawa et al.[34] observed such core−shell structure for block copolymers by microtoming the samples embedded in epoxy resin.

Figure 9a is a micrograph for the (PVPy)−CPB sample with composition of CPB/PVPy 10/1 (w/w) obtained in hexane/chloroform 6/4 (v/v). The sample was observed without staining. The micrograph displays discrete spherical particles with diameters around 40−80 nm. As the particles have relatively clear boundary and their size is much smaller than $\langle D_h \rangle$ from DLS, it is reasonable to ascribe the dark images to the core part of the micelles. The shell is invisible because of its low density and consequently low contrast to the background.

Figure 9b presents the morphologies of the same sample as in Figure 9a but being stained by OsO_4 vapor for 30 min prior to the TEM observations. The stained sample showed quite different morphologies. Each dark sphere is surrounded by a halo which scatters electrons less strongly than the core but more so than the background. Obviously, the halo corresponds to the shell composed of CPB chains which are packed less densely than PVPy in the core but preferentially stained by OsO_4. As there are no clear boundaries either between the shell and core or between the shell and background,

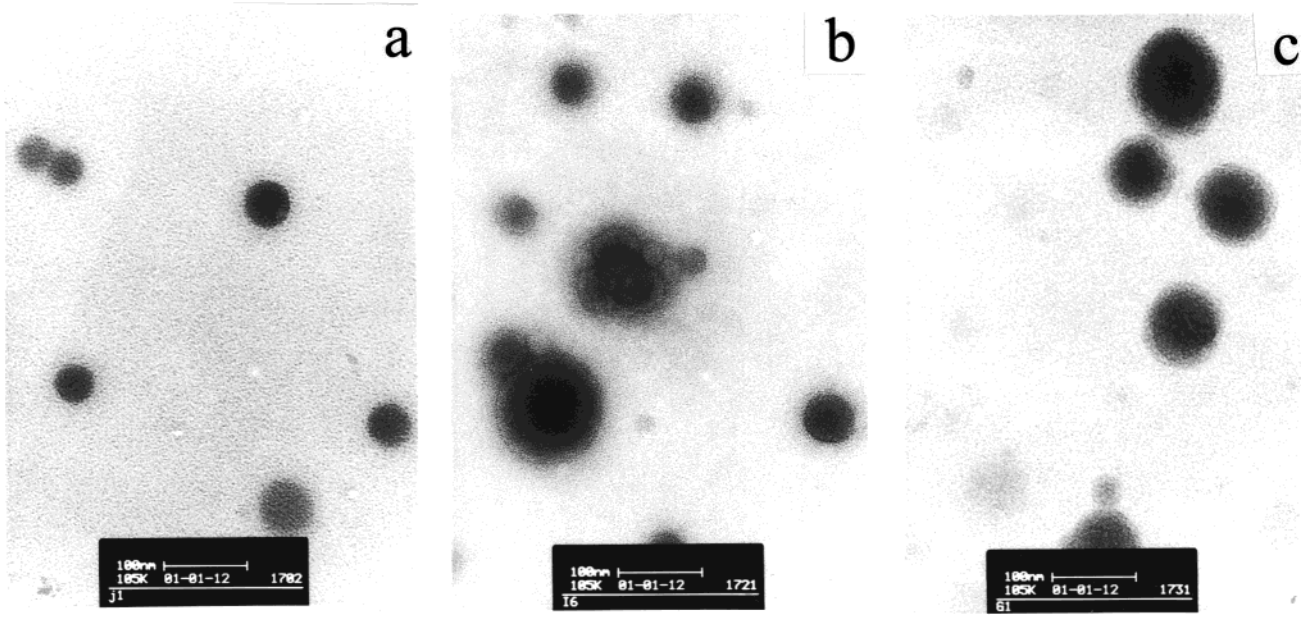

Figure 9. Micrographs of (a) (PVPy)−CPB without staining and (b) stained with OsO_4 for 30 min and (c) (CPB)−PVPy stained for 60 min. The bar ≈ 100 nm.

it is difficult to estimate the precise thickness of the shell. Besides, in the micrograph, clusters consisting of two or three elementary micelles can be seen as well. They were probably formed during the process of the solvent evaporation of the samples on the grid.

Similarly, (CPB)−PVPy in nitromethane/chloroform 6/4 (v/v) without staining did not show any internal structures as the shell part was invisible. However, clear core−shell structure was revealed for the stained samples by OsO_4 for 60 min as shown in Figure 9c. All the particles have a dark core surrounded by a less dense shell. The contrast between the shell and the background has been intensified by staining of PVPy chains.[35] The scattering ability of the shell seems between the core and the background as PVPy chains were stained by OsO_4 to a much lower degree than CPB ones which contain double bonds. Although there is a relatively clear boundary between the shell and background, that between the shell and core is quite diffusive. Only a very rough estimation could be made giving a thickness of the shell around 20 nm.

Because the samples for TEM observations were prepared by evaporation of the dilute micelle solutions on grids, aggregation of the micelle particles, chain collapse, and micelle deformation, etc., cannot be avoided. Therefore, we do not expect to get an accurate size and size distribution of the micelles from TEM in accordance with the DLS results. However, our TEM results do confirm the core−shell structure of the noncovalently connected micelles. Such structure in general does not show any substantial difference from that of the conventional micelle of block or graft micelles.

Precursors for Hollow Spheres. The noncovalently connected micelles, in our opinion, could serve as efficient precursors for producing polymeric hollow nanospheres which are in much demands in various high-tech applications.[36] The procedure includes cross-linking the shell and then removing the core simply by dissolution. This procedure is obviously much simpler than that for conventional micelles, where chemical or biological degradation is necessary in removing the core.[37,38] The related work using the noncovalently connected micelles is in progress in our laboratory.

Acknowledgment. This work was supported by the National Natural Science Foundation of China (NNSFC No. 29992590), the National Basic Research Project-Macromolecular Condensed State Programme. The CPB sample was kindly supplied by Prof. X. Z. Han, The Changchun Institute of Applied Chemistry, China.

References and Notes

(1) Halperin, A.; Tirrell, M.; Lodge, T. P. *Adv. Polym. Sci.* **1992**, *100*, 31.
(2) Webber, S. E. *J. Phys. Chem. B* **1998**, *102*, 2618.
(3) Moffitt, M.; Khougaz, K.; Eisenberg, A. *Acc. Chem. Res.* **1996**, *29*, 95.
(4) Tuzar, Z.; Kratochvil, P. In *Surface & Colloid Science*; Matijevic, E. Ed.; Plenum Press: New York, 1993; Vol 15, p 1.
(5) Harada, A.; Kataoka, K. *Science* **1999**, *283*, 65; *Macromolecules* **1995**, *28*, 5294; *Macromolecules* **1998**, *31*, 288.
(6) Kabanov, A. V. Bronich, T. K.; Kabanov, V. A.; Yu, K.; Eisenberg, A. *Macromolecules* **1996**, *29*, 6797.
(7) Wu, C.; Niu, A.; Leung, L. M. *J. Am. Chem. Soc.* **1999**, *121*, 1954.
(8) Liu, S.; Zhu, H.; Zhao, H.; Jiang, M.; Wu, C. *Langmuir* **2000**, *16*, 3712.
(9) (a) Zhao, H.; Liu, S.; Jiang, M.; Yuan, X.; An, Y.; Liu, L. *Polymer* **2000**, *41*, 2705. (b) Zhao, H.; Gong, J.; Jiang, M.; An, Y. *Polymer* **1999**, *40*, 4521. (c) Yuan, X.; Zhao, H.; Jiang, M.; An, Y. *Acta Chim. Sinca* **2000**, *58*, 118.
(10) Liu, S.; Zhang, G.; Jiang, M. *Polymer* **1999**, *40*, 5449.
(11) Liu, S.; Jiang, M.; Liang, H.; Wu, C. *Polymer* **2000**, *41*, 8697.
(12) Liu, S.; Pan, Q.; Xie, J.; Jiang, M. *Polymer* **2000**, *41*, 6919.
(13) Kikuchi, A.; Nose, T. *Macromolecules* **1996**, *29*, 6770.
(14) Kikuchi, A.; Nose, T. *Macromolecules* **1997**, *30*, 896.
(15) Eckert, A. R.; Webber, S. E. *Macromolecules* **1996**, *29*, 560.
(16) Ma, Y.; Cao, T.; Webber, S. E. *Macromolecules* **1998**, *31*, 1773.
(17) Kosonen, H.; Ruokolainen, J.; Knaapila, M.; Torkkeli, M.; Jokela, K.; Serimaa, R.; ten Brinke, G.; Bras, W.; Monkman, A. P.; Ikkala, O. *Macromolecules* **2000**, *33*, 8671.
(18) Ruokolainen, J.; Tanner, J.; Ikakala, O.; ten Brinke, G.; Thomas, E. L. *Macromolecules* **1998**, *31*, 3532.
(19) Kato, T.; Ihata, O.; Ujiie, S.; Tokita, M.; Watanabe, J. *Macromolecules* **1998**, *31*, 3551.
(20) Kato, T.; Kihara, H.; Ujiie, S.; Uryu, T.; Frechet, J. M. J. *Macromolecules* **1996**, *29*, 8734.
(21) Kato, T.; Nakano, M.; Moteki, T.; Uryu, T.; Ujiie, S. *Macromolecules* **1995**, *28*, 8875.
(22) Ohtake, T.; Ogasawara, M.; Ito-Akita, K.; Nishina, N.; Ujiie, S.; Ohno, H.; Kato, T. *Chem. Mater.* **2000**, *12*, 782.
(23) Chu, B. *Laser Light Scattering: Basic Principles and Practice*, 2nd ed.; Academic Press: London, 1991.

(24) Jiang, M.; Li, M.; Xiang, M.; Zhou, H. *Adv. Polym. Sci.* **1999**, *146*, 121.
(25) Lunberg, R. D.; Phillips, R. R. *J. Polym. Sci., Polym. Phys.* **1989**, *27*, 245.
(26) Feng, K.; Zeng, Z.; Ouyang, W.; Li, Z. *J. Appl. Polym. Sci.* **1996**, *61*, 729.
(27) Pan, Y.; Huang, Y.; Liao, B.; et al. *Eur. Polym. J.* **1998**, *34*, 207, 213.
(28) Lu, X.; Weiss, R. A. *Macromolecules* **1991**, *24*, 5763.
(29) (a) Jiang, M.; Liu, W.; Wu, C.; Woo, K. *Polymer* **1997**, *28*, 405. (b) Liu, W.; Jiang, M. *Chem. J. Chin. Univ.* **1997**, *18*, 309.
(30) Zhu, L.; Jiang, M.; Liu, L.; Zhou, H.; Fan, L. *J. Macromol. Sci., Phys. B* **1998,** *37* (6), 827.
(31) Xiang, M.; Jiang, M.; Zhang, Y.; Wu, C. *Macromolecules* **1997**, *30*, 5339.
(32) Forster, S.; Zisenis, M.; Wens, E.; Antoniette, A. *J. Chem. Phys.* **1996**, *24*, 9956.
(33) Wu, C.; Gao, J.; Li, M.; Zhang, W. M.; Jiang, M. *Macromol. Symp.* **2000**, *150*, 219.
(34) Serizawa, T.; Tekahara, S.; Akashi, M. *Macromolecules* **2000**, *33*, 1759.
(35) Ishizu, K.; Ikemoto, T.; Ichimura, A. *Polymer* **1999**, *40*, 3147.
(36) Jenekhe, S. A.; Chen, X. L. *Science* **1999**, *283*, 372.
(37) (a) Stewart, S.; Liu, G. *Angew. Chem., Int. Ed.* **2000**, *39*, 340. (b) Stewart, S.; Liu, G. *Chem. Mater.* **1999**, *11*, 1048. (c) Ding, J.; Liu, G. *J. Phys. Chem. B* **1998**, *102*, 6107.
(38) (a) Huang, H.; Kowalewski. T.; Remsen, E.; Gertzmann, R.; Wooley, K. L. *J. Am. Chem. Soc.* **1997**, *119*, 11653. (b) Huang, H.; Remsen, E.; Kowalewski. T.; Wooley, K. L. *J. Am. Chem. Soc.* **1999**, *121*, 3805. (c) Zhang, Q.; Remsen, E.; Wooley, K. L. *J. Am. Chem. Soc.* **2000**, *122*, 3642.

MA0105845